Environmental Science Advances

ROYAL SOCIETY OF CHEMISTRY

PAPER

View Article Online
View Journal | View Issue

Cite this: *Environ. Sci.: Adv.*, 2023, **2**, 339

A facile scalable hydrophobic biocomposite for oil spill cleanup

Ramesh Kandanelli and Chinthalapati Siva Kesava Raju *

In this work, we attempt to address the oil spill problem by synthesizing a novel hydrophobic biocomposite material from the readily available lignocellulosic biomass. In this work, saw dust was functionalized using a long alkyl silylating agent post-pretreatment method. The functionalization imparted substantial hydrophobicity and oleophilicity, resulting in the selective absorption of oil from the oil/water mixture. The synthesized biocomposite was characterized by various analytical techniques to confirm functionalization. Furthermore, the biocomposite was utilized to selectively absorb spilled crude oil from oil/water biphasic mixtures. The ease of coagulated mass separation, biocomposite regeneration and recyclability is demonstrated.

Received 22nd July 2022
Accepted 23rd December 2022

DOI: 10.1039/d2va00167e

rsc.li/esadvances

Environmental significance

Oceanic and sea waters have been suffering from oil spills on the water surface caused by spillage, leakage, industrial run offs, dumping *etc.* An immediate remedy for selective oil removal is essential for the sustenance of aquatic plants and animals in addition to the reduction of environmental pollution. The following points are the significant features for mitigating the commonly faced oil spill issues. Simple preparation of a hydrophobic biocomposite by surface modification of biomass. Selective crude oil absorption by the hydrophobic material in an oil/water mixture. Confirmation of hydrophobicity by various analytical techniques. Crude oil recovery and biocomposite recyclability.

Introduction

The ever-growing marine oil spills due to high consumption and oil exploration forecast drastic effects on the environment and all living organisms.[1] To circumvent this issue, a number of methods have been adopted. Traditional methods include *in situ* burning,[2] mechanical separation[3] and bioremediation.[4] However, every method has its own disadvantages including environmental and economic challenges in the current scenario. Recent developments include the usage of absorbent materials for the physical absorption of oil.[5] Novel oil separation materials include phase selective gelators,[6] cellulosic fibers,[7] porous polymeric systems,[8] polysiloxane sponges,[9] carbon based materials,[10] hydrophobic fabrics,[11–13] and coated melamine sponges/foams.[14]

As a result, there have been increasing reports on the development of environmentally friendly materials for containing oil spills. The methods to generate these materials include the incorporation of hydrophobicity on existing absorbents mainly *via* chemical functionalization. Commercially available absorbents, sponges, and fabrics have undergone surface reactions without the loss of absorption capabilities to obtain their hydrophobic and oleophilic nature. More often, the conditions have been non-ambient (freeze drying/lyophilization) and sometimes challenging. Synthesizing high absorbing nano carbon in the form of sponges,[15] tubes,[16] and fibers[17] through chemical vapor deposition is expensive and scaling up becomes nonviable.

The usage of abundantly available lignocellulosic biomass, agricultural residues, and renewable wastes for such environmental applications trigger research towards sustainability and pollution-free atmosphere. Hence, in this work, we have used an easily obtainable biomass, namely saw dust produced as a waste byproduct from wood mills and furniture outlets, as a selective oil absorbing material. One of the reports by Wang *et al.* includes a three-step procedure by nano silica, polyethylene, and a silylating agent in THF (with comparable absorption capacity) for developing superhydrophobic and superoleophilic saw dust.[18] One of the earliest works with a biomass-based sorbent, oleic acid-grafted saw dust, was reported by Jayaram and co-workers.[19] Reports on various biomass-based sorbents are limited to absorption tests of a single type of crude oil and specialty solvents. Testing a range of crude oils using biomass as a selective sorbent has not been fully explored. Herein, we directly functionalized pretreated saw dust using trichlorooctadecyl silane, which was then used for oil absorption straight away. Thus, the prepared sorbent has been given the name high performance hydrophobic biocomposite (HP-HBC) and will be referred as HBC. HBC showed selective crude oil

Analytical and Chemical Synthesis Division, Hindustan Petroleum Green R&D Centre (HPGRDC), KIADB Industrial Area, Devanagonthi, Bengaluru 560067, India. E-mail: cskraj@hpcl.in

absorption, and its regeneration and recyclability have also been demonstrated.

Materials and methods

Saw dust was obtained in Bangalore from a local mill. Sodium hydroxide, hydrogen peroxide (30%), sodium chloride, acetone (AR grade), toluene, xylene, dodecane and hexane were purchased from Merck. Five crude oil samples with varying API (densities) and other refinery distillates [diesel, kerosene, straight run naphtha (SRN)] were obtained from the Crude and Fuel Testing division. The water used in all experiments was from Millipore. For absorption experiments, a 5% sodium chloride solution of Millipore water was prepared to mimic sea water (although the average salt content in sea water is about 3.5%). All absorption tests were done in triplicate, and the average of three values were considered as the sorbent capacities.

Thermogravimetric analysis (TGA). Thermal analysis of sawdust samples were carried out on the SDT750 model from TA instruments, USA. Analysis was carried under N_2 atmosphere with a flow rate of 100 mL per min.

Fourier transform infrared (FTIR). FTIR measurement of the sawdust samples was performed on a Frontier FT-IR spectrometer from PerkinElmer (USA) in ATR mode.

CPMAS NMR (cross polarization magic angle spinning nuclear magnetic resonance). ^{13}C CPMAS NMR of the samples were obtained at a resonating frequency of 125 MHz on a JEOL (Japan) 500 MHz NMR spectrometer. The rotation speed was kept at 12 kHZ, and the temperature during the experiment was constant at 25 °C.

Powder-X-ray diffraction. Samples were characterized by P-XRD measurements on a X'pert3 X-ray diffractometer from Panalytical, Netherlands. Source: Cu K-alpha, 0.15418 nm (Bragg–Brentano geometry).

FE-SEM (field emission scanning electron microscope). FESEM images of sawdust samples were obtained on a JSM-7610F from JEOL, Japan. Samples were sputter-coated with Pd–Pt prior to obtaining better imaging.

Abbreviation for the saw dust samples

PSD: pretreated saw dust; HP-HBC: high performance hydrophobic biocomposite.

Properties of crude oil samples. To widen the scope of HBC for practical application, the absorption tests were conducted against five different types of crude oil samples. Properties of crude oil vary to a large extent depending on the source (geographical location). Key parameters that dictate the basic nature of crude oil, such as the API (American Petroleum Index) number that signifies the specific gravity, and the TAN (Total Acid Number) that indicates acidity, are listed in Table 1.

Pretreatment of saw dust (SD)

Pretreatment was done prior to surface functionalization of the biomass. Saw dust was obtained locally and sieved to obtain uniform particles of about 1 mm. A mass of 100 g of saw dust was weighed and stirred (6 h) in a beaker containing 0.5 wt% NaOH solution (200 mL) and 30% hydrogen peroxide solution (7 mL). Saw dust was filtered and washed with water until the NaOH was absent. Once the pH was close to neutral, the solid was washed with acetone and dried in an oven at 50 °C for 4 hours. The resultant pretreated sawdust was observed to be pale yellow, and was further used for oleophilic treatment.

Table 1 Crude oils and properties

Crude oil	API gravity	TAN
C1	33	0.30
C2	18.82	0.16
C3	27.12	2.87
C4	30.26	0.3
C5	36.1	0.28

Preparation of the hydrophobic biocomposite (HBC)

A mass of 10 g of PSD was suspended into a round bottom flask (250 mL) containing 100 mL of toluene. Dropwise addition of 0.5 mL octadecyltrichlorosilane (5% v/w) was carried out with continuous stirring. The stirring continued for 4 hours, and the modified biomass suspension was subsequently filtered by suction. The modified saw dust was washed with toluene (3 × 25 mL). Later, the hydrophobic sawdust was dried in an oven at 70 °C. The obtained dry HBC was characterized and used for studies.

Absorption studies. In a typical procedure, a beaker with saline water containing a measured amount of crude oil was taken. HBC was sprinkled on the oil layer after its weight was noted. The thus-sprayed HBC was capable of absorbing crude oil in 5–10 s. The filtered mass weight was noted after tearing the mesh's weight. Subsequently, the absorption capacity was calculated.

Results and discussion

The prepared absorbent (HBC) is hydrophobic in nature. The synthesis is presented in Scheme 1. Trioctyl groups make the composite super-oleophilic, which ensures the selective absorption of oil molecules by mainly van der Waals interactions and the inherent porosity of the biomass.

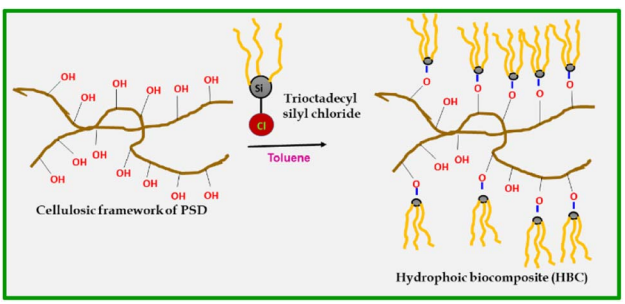

Scheme 1 Functionalization of PSD to BSD.

Absorption studies of HBC with various crude oils

Five crude oil samples having various densities (APIs) were tested for the sorption capacity of the HBC. The procedure for the oil absorption study is mentioned in the Materials and methods' section. A pictorial scheme of an absorption experiment with crude oil (API 17) is shown in Fig. 1. The absorption capacity was calculated by using the equation that was recently reported:[25]

$$C_A = (W_{CM} - W_{HBC})/W_{HBC}$$

C_A: absorption capacity; W_{CM}: weight of the coagulated mass; W_{HBC}: weight of the HBC.

The absorption capacities mainly depended on the API values. The crude oil is less dense with increasing API value. Fig. 2a shows the absorption capacities of crude oils by HBC. Among the tested crude oils, the light ones C1 and C5 of comparable API values showed absorption capacities of 18 and 16, respectively. Crude oils C3 and C4 are medium dense crude oils (as per their API values) that show absorption capacities of 10 and 9, respectively. Crude C2 had the lowest API, signifying that it is the densest of all, and it was the least absorbed with a capacity of 8. Table 2 gives a comparison of the various biomass-based absorbent capacities from various reported results in the literature.

Apart from crude oils, solvents and refinery distillates were tested for selective absorption by HBC. Expectedly, the neat oils showed higher average absorption capacities than the crude oils. The studies showed that the absorption was relatively higher for the aliphatic hydrocarbons compared to that of aromatic solvents. The highest absorption capacity of 20 was observed for straight run naphtha (SRN), a light refinery distillate (boiling range, 35–180 °C). Hexane and C12–C14 (kerosene) fractions were absorbed 18 times by HBC, followed by dodecane and diesel fractions that showed 15 times absorption. Toluene and xylene showed absorption capacities of 14 and 12 times, respectively. The absorption values are summarized in Fig. 2a, and the schematic for the diesel absorption and separation is shown in Fig. 3.

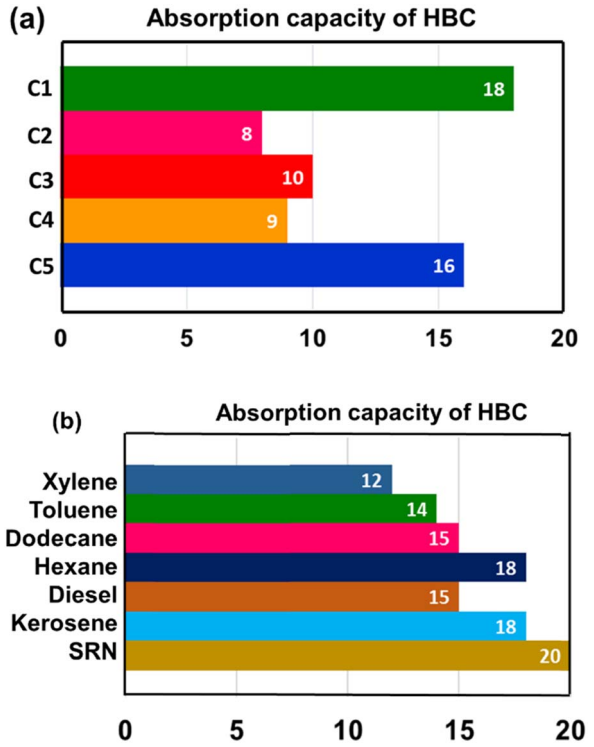

Fig. 2 (a) Crude oil absorption capacities of HBC, (b) model solvents and refinery distillates' absorption; *absorption capacity value is g of oil absorbed per g of HBC.*

Hydrophobicity of HBC

The key aspect of the powder sorbent (HBC) is its repellent nature towards water, which makes it highly selective in the absorption of oil media. To confirm the hydrophobicity, a water droplet was placed on non-modified sorbent and HBC. The formed visible contact angle is greater on HBC than on the non-functionalized biomass. The water droplet that is placed on HBC does not sink in at all and occupies the least volume shape of a sphere on the surface, revealing the hydrophobic nature of HBC. Whereas, the water droplet placed on PSD readily goes into the fibers. Fig. 4a depicts the hydrophobicity of HBC.

Recovery of crude and recyclability of HBC

It also becomes important when it comes to the recovery of the crude oil that is coagulated along with HBC. A kero fraction was taken to wash the dark pulp through the mesh. The immobilized crude oil gets washed off through the mesh, leaving

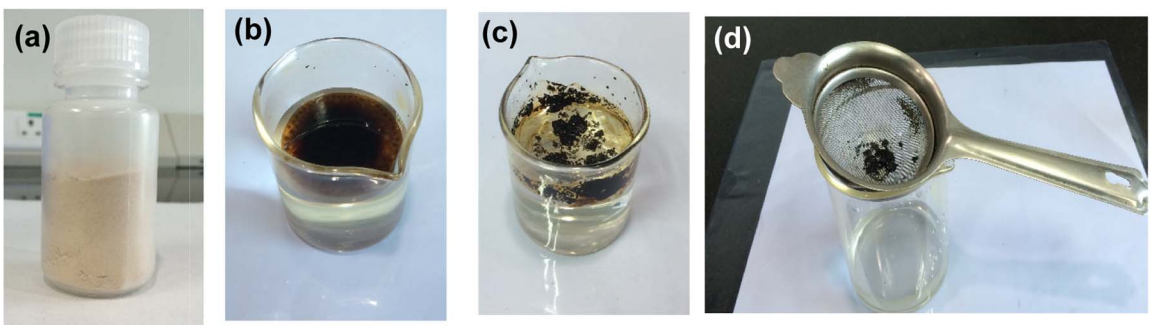

Fig. 1 (a) HBC, (b) crude oil (C2) placed on water, (c) crude oil absorption by HBC, and (d) separation of the congealed mass by simple filtration.

Table 2 Comparison of the absorption capacities with the reported biomass-based sorbents

Absorbing material	Absorption capacity g of oil/g of sorbent	Ref.
HBC	18	Present study
Oleic acid grafted saw dust	6	19
Superoleophilic corn straw	20	20
Hydrolysis lignin	2	21
Acetylated rice husk	10.3	22
Heat-treated rice husks	16	23
Saw dust–bentonite–$Ca(OH)_2$ mixture	16	24
Dodecyl gallate cornstalk pitch	46.4	25

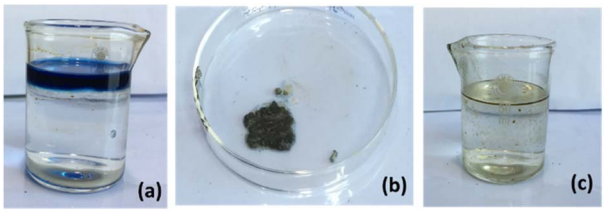

Fig. 3 (a) Diesel (dyed in blue) on water, (b) separated diesel coagulated HBC, and (c) water after diesel-HBC clot removal.

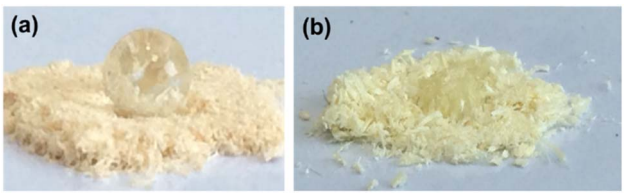

Fig. 4 (a) Water droplet placed on a layer of HBC. (b) Water droplet placed on a layer of PSD.

behind HBC. The obtained HBC after a hexane wash was oven dried at 60 °C. The dried HBC was reused for crude oil absorption. Fig. 5 shows the process of recovery of the crude oil and regeneration of HBC.

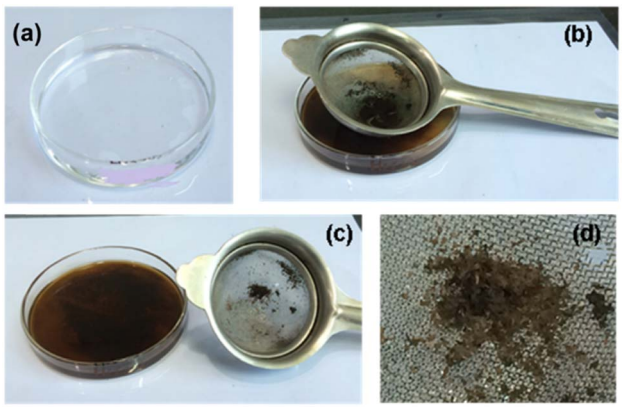

Fig. 5 (a) Kero distillate. (b) Filtered-coagulated mass soaked in kero. (c) Crude recovery from the mass. (d) Regenerated sorbent.

Reusability of HBC

The regenerated sorbent was tested for reusability for absorption studies. A similar procedure to the one performed with the first cycle of coagulation was followed. The sorbent was recovered again by washing with hexane. Usage of regenerated saw dust was carried out for 5 times with a loss of about 10% efficiency for the highest API (least dense) crude oil (Fig. 6a). The recyclability dropped to 3 times in the case of the lowest API (heaviest) crude oil (Fig. 6b). For recycling, the same amount of washing solvent (hexane) that was used the first time was used for the recovery for optimization. Washing with fresh solvent might further increase the recyclability.

Characterization

To confirm the hydrophobic functionalization on HBC, HBC and PSD (pretreated saw dust) were characterized by various techniques. FTIR spectra are shown in Fig. 7. The vibrational stretching bands of OH around 3300 cm^{-1} were observed in both HBC and PSD, suggesting that not all of the free OH groups in hemicellulose or cellulose are silylated.

Notably, a substantial difference in the C–H stretching was observed with high transmission bands at 2917 cm^{-1} and 2849 cm^{-1} in HBC, confirming the presence of a long chain hydrocarbon layer on HBC. Considering the ring steric factors, it was apparent that only the primary hydroxyl, *i.e.*, C6–OH of the sugar backbone might be functionalized. Other common signatures, such as the C–C ring stretching at 1467 cm^{-1} and C–O stretching at 1032 cm^{-1}, were observed.

Fig. 8 shows the ^{13}C CP-MAS NMR spectra of HBC and PSD. Distinguishable functionalization was confirmed during the comparison of two samples. A small peak at 105 ppm indicates the presence of an aromatic backbone that is part of the lignin framework. Peaks in the range of 65–90 ppm belong to carbons

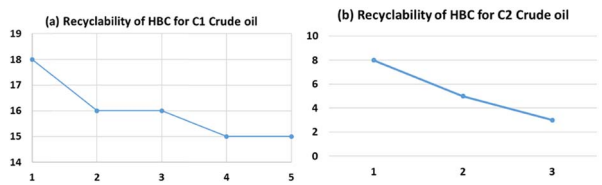

Fig. 6 HBC recyclability with (a) C1 and (b) C2.

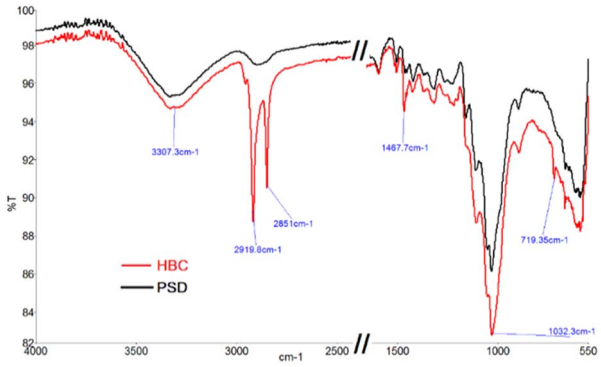

Fig. 7 FTIR spectra of PSD and HBC.

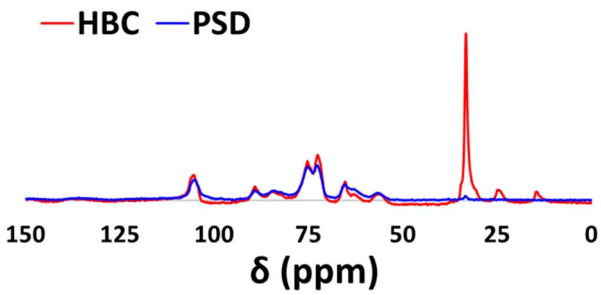

Fig. 8 ^{13}C CP-MAS NMR spectra of HBC and PSD.

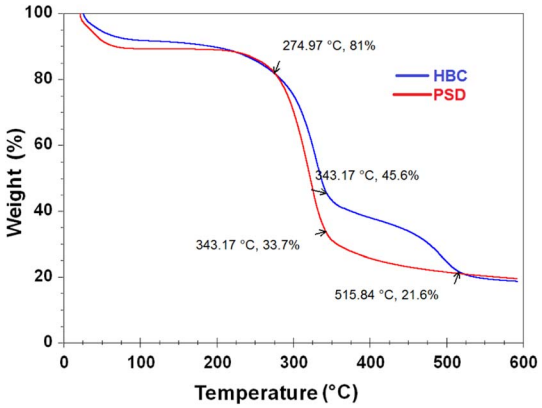

Fig. 9 TGA graph of HBC and PSD.

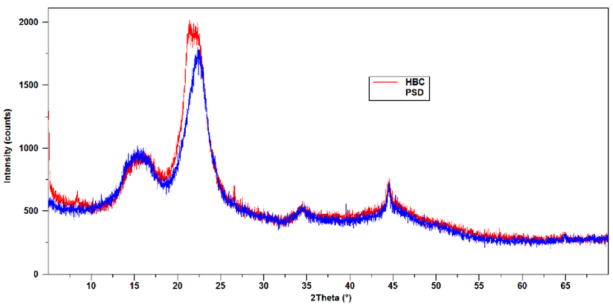

Fig. 10 XRD patterns of PSD and HBC.

with C–O functionality (C1, C2, C3, C4, C5) that are present in the sugar polymer. The C6 carbon that has C–O–Si linkage is shifted slightly from 55 to 52 ppm in HBC compared to that of PSD. Additional peaks of carbons from the long hydrophobic tail were noticeable at 28–30 ppm (internal CH_2 groups), 23 ppm (CH_2 linked to CH_3) and 12 ppm (CH_3), which further validated the presence of long alkyl chains on the composite.

Thermograms of HBC and PSD were obtained in the temperature range of 25 to 600 °C. The measurement was conducted in an oxygen-free atmosphere to observe the decomposition. Disintegration of the samples is depicted in Fig. 9. The thermal degradation profiles suggest that the incorporation of hydrophobicity influences the thermal stability of the material. The weight loss took place in two stages in the case of PSD, whereas it was in three stages in the case of HBC. Volatiles and residual moisture desorbed in the range of 70–120 °C. The second stage decomposition started around 275 °C, where the hydroxyl functionalities start to go off until 345 °C, and everything is degraded in the case of PSD with only the residual carbon left. In the case of HBC, the hydrophobic coating is retained for a longer time until the temperature reaches around 480 °C, and decomposes gradually in the range of 485–515 °C. This suggested the increased thermal stability due to the incorporation of hydrophobic functionalization.

XRD measurements were conducted on both PSD and HBC to determine the differences in the lattice packing. Diffractograms of PSD and HBC are shown in Fig. 10. PSD showed characteristic diffraction peaks of cellulose reflections at 2θ values of 16.5° (101), 18° (101), 22.6° (002), 34.7° (040), and 44.5°. The intense diffraction peak at 22.6 corresponds to the crystalline planes that comprise the packing of molecules due to the intermolecular hydrogen bonding between two immediate cellulosic molecules. The C6 primary hydroxyl is involved in H-bonding with C2–OH of the adjacent glucose unit, as well as C3/C2–OH of glucose in the neighboring cellulose molecule.[24] During pre-treatment, the biomass is softened. In the process, the H-bonding of C6–OH is disrupted to a significant extent and becomes accessible to get functionalized. The XRD pattern in HBC shows the peak splitting of the (040) plane at 2θ at 22.6°, suggesting that packing may be slightly rearranged due to functionalization. As a result, a doublet is observed. However, there were no major shifts and changes observed for the other reflections.

The morphological details of both PSD and HBC were obtained by FESEM. Distinct features in the topographies pre- and post-hydrophobicity incorporation were noticed. Images from PSD are shown in Fig. 11a and b. They reveal a strong fibrous network entangled extensively throughout the sample. The fiber diameter was in the range of 20–30 nm, which is the typically obtained dimension for microfibrillated cellulose fibers prepared by various pretreatment methods.[25] On the other hand, the morphology is entirely different post-functionalization. The fibrous topography is no longer evident in HBC [Fig. 11c and d]. The high-resolution images of HBC resembled a particulate kind of landscape with a rough surface on the top.

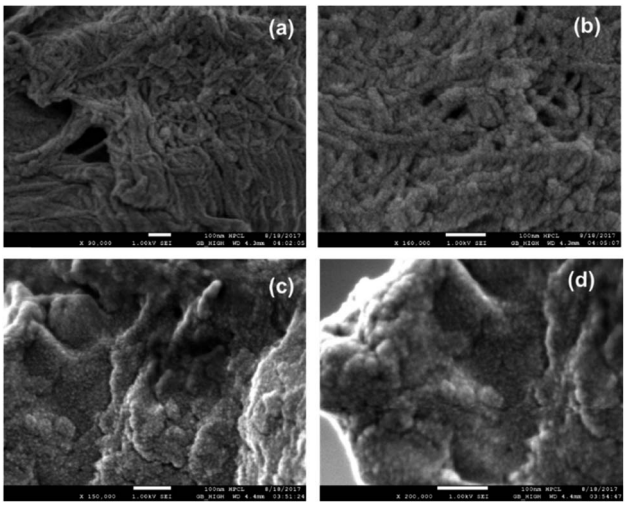

Fig. 11 SEM images of (a and b) PSD; (c and d) (scale: 100 nm).

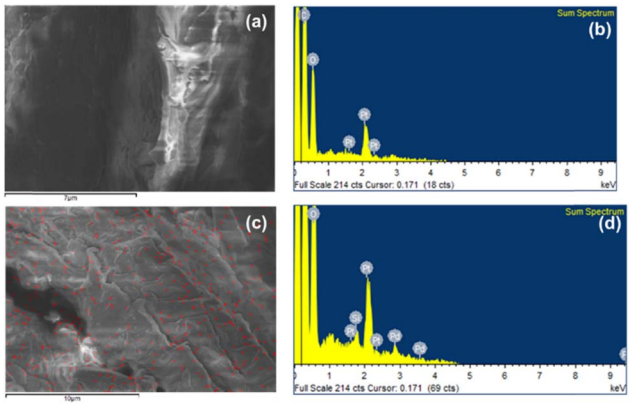

Fig. 12 Mapped areas of (a) PSD and (c) HBC; elemental data of (b) PSD and (d) HBC.

The elemental identifications of PSD and HBC were obtained by Energy Dispersive Spectroscopy through FESEM. Fig. 12a and c show the areas from which the elemental analysis of both PSD and HBC, respectively, were extracted. The compositional distribution revealed a large presence of C, O expectedly in both the samples. Pt was observed due to sputter coating, which is used for enhancing conductivity of the sample.

Additionally, Fig. 12c indicates a uniform silicon distribution (assigned red color) in the area scanned. This is also reflected in the subsequent hydrophobicity. Fig. 12b and d show the elemental identification by binding energy values, which is also confirmed by that extra peak of silicon at 1.8 keV in HBC.

Conclusions

In this manuscript, we have developed a novel hydrophobic biocomposite (HBC) using a wood waste at ambient conditions. The thus-prepared material showed selective absorption of various types of crude oil from oil/water mixed media. The absorption capacity mainly depended on the density of the crude oil. As part of the study, even organic solvents and widely produced refinery distillates were also studied for absorption. A detailed characterization by various techniques like CPMAS, FTIR, EDS (FESEM) and TGA confirmed the hydrophobic functionalization. We believe this novel alternative shows a huge potential for oil spill remedy at a practical scale. One kilogram of HBC has been prepared to demonstrate the feasibility to scale up. Efforts are in process to minimize the steps for washings and for increased scale up.

Conflicts of interest

The authors declare no conflicts of interest.

Acknowledgements

Crude and Fuel Testing Division, Corporate R&D HPCL, is acknowledged for providing the crude oils of different APIs along with refinery distillates. The support and encouragement from the HPCL Management is gratefully acknowledged.

Notes and references

1 Y. Samiullah, *Oil Petrochem. Pollut.*, 1985, **2**, 235–264.
2 J. V Mullen and M. A. Champ, *Spill Sci. Technol. Bull.*, 2003, **8**, 323–330.
3 V. Broje and A. A. Keller, *Environ. Sci. Technol.*, 2006, **40**, 7914–7918.
4 S. J. Varjani, *Bioresour. Technol.*, 2017, **223**, 277–286.
5 R. K. Gupta, G. J. Dunderdale, M. W. England and A. Hozumi, *J. Mater. Chem. A*, 2017, **5**, 16025–16058.
6 C. S. K. Raju, B. Pramanik, R. Ravishankar, P. V. C. Rao and G. Sriganesh, *RSC Adv.*, 2017, **7**, 37175–37180.
7 S. Wang, X. Peng, L. Zhong, J. Tan, S. Jing, X. Cao, W. Chen, C. Liu and R. Sun, *J. Mater. Chem. A*, 2015, **3**, 8772–8781.
8 J. Saleem, A. Bazargan, J. Barford and G. McKay, *Chem. Eng. Technol.*, 2015, **38**, 482–488.
9 S. Zhang, J. Guo, X. Ma, X. Peng, Z. Qiu, J. Yinga and J. Wang, *New J. Chem.*, 2017, **41**, 8940–8946.
10 S. Gupta and N.-H. Tai, *J. Mater. Chem. A*, 2016, **4**, 1550–1565.
11 H. Yu, M. Wu, G. Duan and X. Gong, *Nanoscale*, 2022, **14**, 1296–1309.
12 Z. Xiong, J. Huang, Y. Wub and X. Gong, *Nanoscale*, 2022, **14**, 5840–5850.
13 Y. Nie, S. Zhang, Y. He, L. Zhang, Y. Wang, S. Li and N. Wang, *New J. Chem.*, 2022, **46**, 4734–4745.
14 Y. Yang, Y. Deng, Z. Tonga and C. Wang, *J. Mater. Chem. A*, 2014, **2**, 9994–9999.
15 X. Ge, W. Yang, J. Wang, D. Long, L. Linga and W. Qiao, *RSC Adv.*, 2015, **5**, 70025–70031.
16 K. Zhu, Y.-Y. Shang, P.-Z. Sun, Z. Li, X.-M. Li, J.-Q. Wei, K.-L. Wang, D.-H. Wu, A.-Y. Cao and H.-W. Zhu, *Front. Mater. Sci.*, 2013, **7**, 170.
17 B. Wang, R. Karthikeyan, X.-Y. Lu, J. Xuan and M. K. H. Leung, *Ind. Eng. Chem. Res.*, 2013, **52**, 18251–18261.
18 D. Zang, F. Liu, M. Zhang, Z. Gao and C. Wang, *Chem. Eng. Res. Des.*, 2015, **102**, 34–41.

19 S. S. Banerjee, M. V. Joshi and R. V. Jayaram, *Chemosphere*, 2006, **64**, 1026–1031.
20 Y. Xu, H. Yang, D. Zang, Y. Zhou, F. Liu, X. Huang, J. Chang, C. Wang and S.-H. Ho, *Bioresources and Bioprocessing*, 2018, **8**(1–13), 5.
21 H. Po, S. Tatsiana, R. Ivan, H. Dzmitry, T. Nadejda, T. Galina and A. Alexandr, *Adv. Biosci. Biotechnol.*, 2016, **7**, 501–530.
22 N. E. Thompson, G. C. Emmanuel, K. J. Adagadzu and N. B. Yusuf, *Arch. Appl. Sci. Res.*, 2010, **2**, 142–151.
23 K. K. Kudaybergenov, E. K. Ongarbayev and Z. A. Mansurov, *J. Pet. Environ. Biotechnol.*, 2015, **6**, 1–3.
24 T. Sun and D. D. L. Chung, *J. Environ. Eng.*, 2013, **139**, 1470–1481.
25 D. Peng, W. Li, X. Liang, L. Zheng and X. Guo, *J. Environ. Sci.*, 2023, **124**, 105–116.